Development of Compact and Lightweight Stand-up Powered Wheelchair — Fall Risk Analysis When at Rest and Decelerating

Tomozumi Ikeda, Toshitake Araie, Akira Kakimoto, and Koji Takahashi

***Abstract*—When unassisted walking is difficult, a wheelchair with a stand-up function enables a standing position as well as a sitting position for work and improved convenience. However, in the standing position, the center of gravity is high, and to prevent falling it is common to shorten the long wheelbase of the wheelchair, or to lower its center of gravity. It is also desirable to reduce the size and weight of the wheelchair for space and portability reasons. Therefore, we aim to reduce the size and weight of electric wheelchairs that can move with a stable high attitude by providing a fall-prevention control function. This study reports on the appearance and the dimensions of a prototype stand-up powered wheelchair and the results of a fall risk analysis when at rest and decelerating.**

***Index Terms*—Stand-up powered wheelchair, falling mechanism, fall risk analysis, seat-lift mechanism, wheelchair electric unit.**

I. Introduction

It is suggested that wheelchair users often experience painful and secondary complications due to long-term sitting.

Standing is an effective way to counterbalance the physical or mental negative effects of constant sitting. Standing has beneficial effects on body functions and structures such as maintaining bone mineral density, improving circulation, improving range of motion, etc. In addition, a standing position can give wheelchair users a sense of confidence and equality through face-to-face communication with a non-disabled person, and can improve functional reach to enable participation in other activities of daily living [1]-[3].

Currently, stand-up wheelchairs have been researched and developed. LEVO, F5corpusVS, etc., are representative commercially available equipment [4]-[7], and they typically have changing body position functions such as reclining, tilting, and seat-lifting. Users can move and work in any posture from standing to sitting. However, because the center of gravity (CoG) in the standing posture is high, these wheelchairs have been traditionally made with a low CoG and long wheelbase to prevent falling down. Further, the following issues of stand-up wheelchairs have been pointed out by Suzuki *et al*. [8]:

- When changing posture, the user's body slides off the backrest or chair, and this rubbing may cause tenderness.
- To maintain attitude, a load is applied on the arm or armpit when changing posture, and on the user's lower limbs when standing.
- Because the user's body is fixed by the fall prevention belt, the user feels a sense of pressure or restraint.

Therefore, it is desirable to reduce the size and weight of the wheelchair from the viewpoint of space and portability, and to ease physical loading when changing position.

The purpose of this study is to develop a compact and lightweight stand-up powered wheelchair equipped with a fall-prevention control function. The wheelchair, which is a welfare tool that supports independent social participation, must have sufficient safety. In order to ensure the stability of the wheelchair, it is necessary to analyze and evaluate the fall risk factors (e.g. the user's body characteristics and posture, the inclination angle of the surface, the seat height, and the amount of acceleration/deceleration). This study provides the configuration of the prototype wheelchair and the fall risk analysis.

II. Falling Mechanism

Fig. 1 depicts a side view of a stand-up wheelchair model. The global coordinate system is O_X-$_Z$, the wheelchair coordinate system is $O_{x\text{-}z}$, the front wheel contact point is F, and the rear wheel contact point is R.

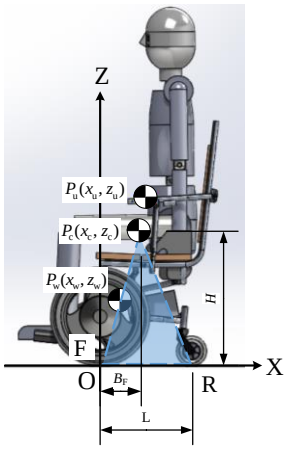

Fig. 1. Model of stand-up wheelchair and user

Denoting the mass and CoG of the user as m_u and P_u (x_u, z_u), the mass and CoG of the stand-up wheelchair as m_w and P_w (x_w, z_w), and the wheelbase as L, the total CoG, P_c (x_c, z_c), is as follows:

$$x_c = \frac{m_u x_u + m_w x_w}{m_u + m_w} \quad (1)$$

Manuscript received April 20, 2019; revised July 23, 2019.

T. Ikeda, T. Araie, A. Kakimoto, and K. Takahashi are with the Polytechnic University of Japan, 2-32-1 Ogawa-nishimachi, Kodaira-shi, Tokyo, Japan (e-mail: ikeda@uitec.ac.jp, araie@uitec.ac.jp, kakimoto@uitec.ac.jp; k-takahashi@uitec.ac.jp).

DOI: 10.7763/IJMO.2019.V9.731

$$z_c = \frac{m_u z_u + m_w z_w}{m_u + m_w} \quad (2)$$

With a posture change from sitting to standing, x_c approaches the origin O and z_c moves in the + z direction. Here, the height H of the triangle from the CoG to the F-R baseline (ΔPFR) is z_c, and the distance between point F and point Pc is $B_F(=x_c)$. Using this model, this study reports on the fall mechanism on a slope when at rest and while decelerating.

A. Fall Mechanism on Slope at Rest

Fig. 2 shows the geometric model at rest. On a horizontal surface as shown in Fig. 2(a), the model is stable if x_c is within the wheelbase L. On a descending surface of angle θ as shown in Fig. 2(b), the CoG point P_c (x_c, z_c) is obtained from the following equations.

$$x_c = B_F \cos\theta - H \cos\left(\frac{\pi}{2} - \theta\right) \quad (3)$$

$$z_c = B_F \sin\theta + H \sin\left(\frac{\pi}{2} - \theta\right) \quad (4)$$

Thus, the wheelchair is stable if x_c is $L\cos\theta \geq x_c \geq 0$.

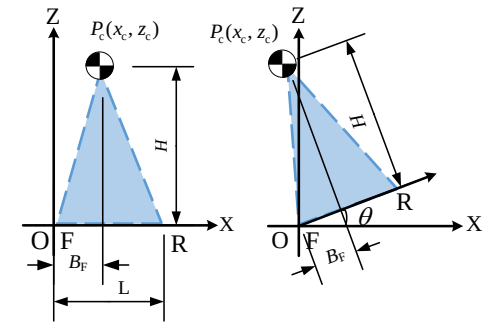

(a) Horizontal surface (b) Descending surface

Fig. 2. Geometric model at rest.

B. Fall Mechanism When Decelerating

An inertial force is applied to both user and wheelchair when accelerating and braking. Assuming that the total mass of the user and wheelchair is M, gravity acceleration is g, and the acceleration of wheelchair is a, the resultant force consisting of the gravity force Mg and the inertia force Ma is applied to point P. In Fig. 3, when this vector lies outside △PFR, the wheelchair falls over.

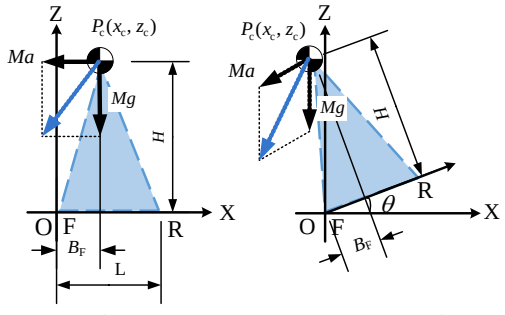

(a) Flat surface (b) Descending surface

Fig. 3. Geometric model when braking.

Deceleration on a flat surface is

$$a \leq \frac{g \cdot B_F}{H}, \quad (5)$$

and deceleration on a descending surface is

$$a \leq \frac{g \cdot B_F}{H}\cos\theta - g \cdot \sin\theta \cdot \quad (6)$$

The following equation defines the deceleration limit:

$$a = \frac{g \cdot B_F}{H} \cdot \quad (7)$$

III. Compact and Lightweight Stand-up Powered Wheelchair

The appearance of the prototype wheelchair is shown in Fig. 4. The design concept of the wheelchair is as follows:

1) The user is an adult with a paralyzed lower limb (height 172 cm, weight 65 kg).
2) The seat can be set to any height.
3) The wheelchair can be carried by two persons, and the mass is 48.6 kg or less.

The maximum dimensions of the electric wheelchair are 1200 mm length, 700 mm width, and 1090 mm heighzt, and the minimum rotation diameter is 1400 mm. The maximum speed of a medium speed electric wheelchair is 6 km/h. These specifications conform to the dimensions and maximum speed defined by Japanese Industrial Standards (JIS).

4) In order to satisfy the above items, the posture range is a range between sitting and half standing.

The prototype wheelchair consists of a body frame made of aluminum, a seat-lift mechanism, a wheelchair electric drive unit including a joystick, and a safety, measurement, and control unit. To ensure accessibility, the drive system of the wheelchair is front wheel drive with two fall prevention wheels and one rear wheel.

Fig. 4. Appearance of the prototype wheelchair.

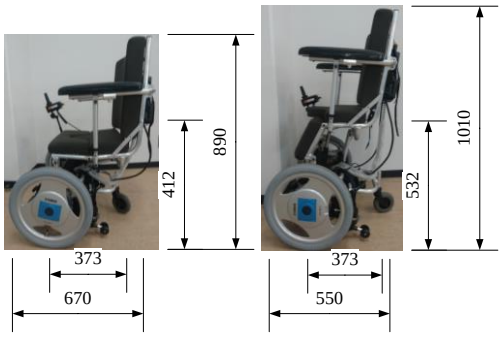

(a) Sitting (b) Standing

Fig. 5. Dimensions of the prototype wheelchair.

The dimensions of the prototype wheelchair are shown in Fig. 5, and a specification is given in Table I. It is 670 mm long, 890 mm tall, 412 mm seat height in the sitting position, and 550 mm long, 1010 mm tall, and 532 mm seat height in a half-standing posture. Regardless of seat height, the width is 660 mm, the wheelbase is 373 mm, the minimum rotation diameter is 910 mm, and the caster trail is 45 mm. The battery is installed behind and below the seat. The mass of the wheelchair electric unit is 14.7 kg, and the total mass including the battery is 32.7 kg. A usage example of the prototype wheelchair is shown in Fig. 6. The user can approach a piece of office equipment and easily operate the control panel owing to the compact design of the wheelchair.

TABLE I: SPECIFICATION OF THE PROTOTYPE WHEELCHAIR

Item		Rating
Length (Sitting～Standing)	[mm]	670~550
Width	[mm]	660
Height(Sitting～Standing)	[mm]	890~1010
Wheelbase	[mm]	373
Seat width	[mm]	435
Backrest angle	[°]	12
Mass of wheelchair electric unit	[kg]	14.7
Total mass (include battery)	[kg]	32.7
Battery		2.9 kg/24 V × 6.7 Ah
Minimum rotation diameter	[mm]	910
Front wheel diameter	[inch]	16
Rear wheel diameter	[mm]	Φ125 × 30

TABLE II: COMPARISON OF THE PROTOTYPE WHEELCHAIR WITH OTHER WHEELCHAIRS

Name	Length [mm] Width [mm]	Minimum turning circle [mm]	Mass [kg]
Prototype wheelchair	550～670 660	910	32.7
LEVO C3 *1	1050 630	1100	185
F5corpusVS *2	1150～1200 660～790	1524	196
RODEM TRI *3	900 680	900	unkown

*1 https://www.levo.ch *2 http://www.permobilkk.jp/
*3 http://www.micotech.jp/

Table II shows the comparison between the prototype and commercially available wheelchairs. The length of the prototype wheelchair is approximately half that of the commercial wheelchairs, and the mass is about one-fifth as much. Thus, the prototype wheelchair is smaller and lighter than commercial wheelchairs.

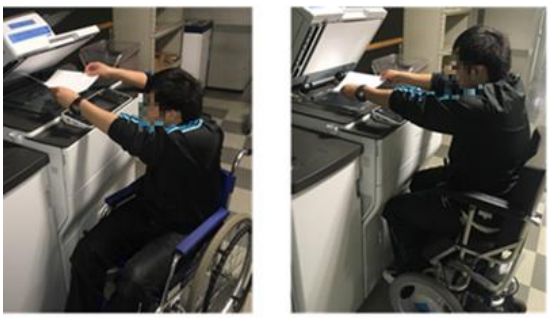

(a) Common wheelchair (b) Prototype wheelchair
Fig. 6. Usage example.

A. Seat-lift Mechanism

A seat-lift mechanism consists of a five-joint linking mechanism, a linear actuator (LA28: LINAK), a control box (CB8-A: LINAK) and a handset (HB40: LINAK). Fig. 7 shows the movement of the link mechanism. In order to avoid a frontward slipping of the buttocks during posture conversion and to reduce the burden on the body by sharing the load between the lower legs and the seat, the seat is a folding type that can be broken approximately in half. During lift, the front seat part bends downward, and the rear seat part maintains an almost horizontal level. The user's posture is a half-standing position at the maximum seat height. The rod of the linear actuator expands and contracts when buttons on the handset are pressed, thus raising and lowering the seat. The lifting time to a seat height from 412 to 532 mm is approximately 12 seconds.

Fig. 7. Movement of the seat-lift mechanism.

B. Wheelchair Electric Unit

A Joy Unit X PLUS (Yamaha Motors) is used as a wheelchair electric unit. The unit has functions of setting speed, acceleration, deceleration, etc. according to the user's purpose. The specification of the wheelchair electric unit is shown in Table III. The "Academic pack," a kit for research and development of Yamaha electric wheelchairs, is used as an operation device. By sending a request command from the external control device to the Academic pack, it is possible to rotate wheels, or acquire internal information such as wheel rotation speed and joystick operation amount.

TABLE III: SPECIFICATION OF JOY UNIT X PLUS

Item			Rating
Mass		[kg]	14.7
Continuous travel distance		[km]	16
Speed	Forward	[km/h]	1.7～5.7
	Backward		0.9～2.8
Load capacity		[kgf]	125

(https://www.yamaha-motor.co.jp/)

C. Safety, Measurement, and Control Unit

Figure 8 shows a functional block diagram of the safety, measurement, and control unit. This unit consists of an integrated controller, a seat-height detection sensor, and a motion sensor. The linear actuator is controlled by the operation buttons on the handset. Handset operation signals are input to the integrated controller, and when there is a risk of falling, the signals are limited.

The linear actuator of the seat-lift mechanism does not have a built-in sensor. Accordingly, the seat height is calculated from the frame dimensions, using the angle between the body frame and the seat-lift mechanism frame. An angle sensor uses a potentiometer (CP-2FABSJ: Midori Precisions) with a built-in return spring for self-restoration of the shaft rotation. The output voltage of the potentiometer V_{out} is converted into digital data using a 10-bit A/D converter

(MCP3008: Microchip). The digital data is fed to the integrated controller.

The seat height h [mm] is obtained from the following equation:

$$H_z = -7.93V_{out}^2 - 18.96V_{out} + 540.88 \cdot \quad (8)$$

A nine-axis sensor (MPU-9150: InvenSense) mounted with a three-axis accelerometer, a three-axis gyro sensor, and a compass, is used for measuring traveling acceleration and vehicle inclination angle.

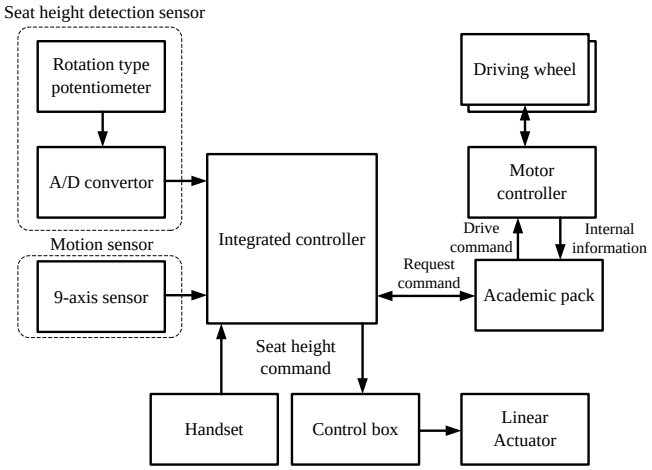

Fig. 8. Functional block diagram of safety, measurement, and control unit.

An integrated controller (Raspberry Pi2 Model B) is used for communication with the Academic pack and for signal processing of various sensors. When the user's request is a "satisfied no-fall" condition, that is, the result of the command will not produce a fall, the integrated controller outputs the request. Alternatively, when the user's request is a "satisfied fall" condition, the integrated controller outputs a command that satisfies the stability condition.

IV. Fall Risk Analysis

The CoG of the prototype wheelchair was estimated from a 3D model created using the 3D CAD design software SOLIDWORKS. In the sitting position, x_w was located 95 mm forward of the center of the wheelbase, and z_w was 274 mm from the floor. In the standing position, x_w moved forward approximately 16 mm, and z_w moved approximately 15 mm upward from the sitting position.

Usually, the CoG of an adult in the standing position is about 56% of the height from the floor, and its position always changes depending on posture and movement. In this study, the CoG of the user was calculated using a mathematical model estimation method [9]. We present the results of a fall risk analysis for three healthy men (A: Height 169 cm, Weight 80 kg, B: Height 178 cm, Weight 60 kg, C: Height 164 cm, Weight 67 kg).

The experiment obtained informed consent from all participants, and proceeded with consideration for safety.

A. At Rest

While the prototype wheelchair was stopped, with a user sitting on a descending surface at 0° or 10°, the center of gravity x_c to the seat height was measured. Fig. 9 shows the CoG x_c to the seat height h for each inclination angle θ.

On a horizontal surface (θ = 0°), the calculated and measured CoG x_c was located within the base of support at all seat heights. On a descending surface (θ = 10°), the calculated CoG x_c was outside the base of support at seat heights of 484 to 532 mm. However, the measured CoG x_c was within the base of support at all seat heights. Despite this result, because the measured value of seat height at 532 mm is near the boundary of the stable region, the wheelchair may fall.

It is thought that the difference between the calculated and the measured values is due to the posture of the body or the contact position of the buttocks.

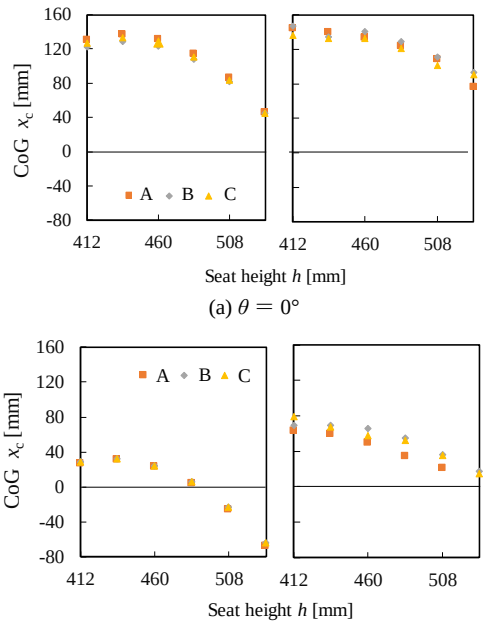

(a) θ = 0°

(b) θ = 10°

Fig. 9. CoG x_c vs. seat height on descending surface. Left: calculated value, Right: measured value.

B. Decelerating

We observed the contact state between the wheel and the surface when decelerating the wheelchair. Figure 10 shows the relationship of the deceleration limit to the seat height and the result of the state of the wheelchair at braking for the three users. The state where all wheels were grounded is shown as a green round symbol; the state where the rear wheel floated is shown as a yellow round symbol; and the state where the rear wheel does not restore is shown as a red round symbol; the stoppage state was determined by observation. In addition, the symbols in Fig. 10 indicate the most unstable state among the three users.

At a deceleration of 0.8 m/s^2, all of the wheels of the prototype wheelchair were in contact with the ground at all seat heights, and the wheelchair was able to stop safely. Near the deceleration limit, the prototype wheelchair did not fall, but, at seat heights other than 532 mm, the rear wheel floated during deceleration and restored to the surface after stopping.

When braking, it is necessary not only to stop a wheelchair stably but also to stop at a short distance while securing the user's comfort. According to JIS and the deceleration of a car that stops smoothly, the braking deceleration range is 1.96–0.93 m/s^2. We found that the decelerating range based

on the experimental results was 2.2–0.93 m/s^2 at seat heights other than 532 mm.

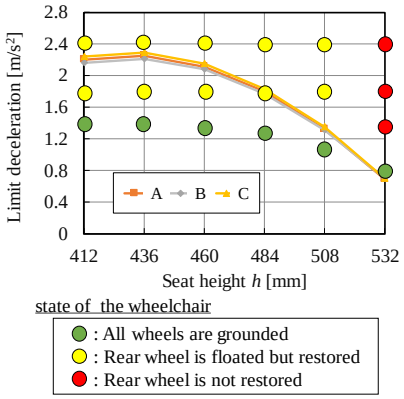

Fig. 10. Deceleration limit (curve) vs. seat height and the resulting most unstable states of the wheelchair at braking for three users.

V. Conclusion

This study presents an overview of a prototype stand-up electric wheelchair and the results of a fall risk analysis at rest and deceleration. It was found that the fall restraint condition of the wheelchair limited the movable range of the seat height to 412–484 mm on a descending surface of 10° at rest, and the deceleration at braking to 2.2–0.93 m/s^2 at seat heights less than 532 mm. In the future, other fall causes such as turning and handling steps will be analyzed and evaluated. Further, an algorithm for fall prevention will be constructed based on the result of the fall risk analysis, and added to the prototype wheelchair.

Acknowledgment

This work was supported by Koya System Design Co.

References

[1] J. Arve, G. Paleg, M. Lange, and J. M Lieberman, "RESNA position on the application of wheelchair standing devices," *Assistive Technology*, vol. 21, pp. 161-168, 2009.

[2] H. Ogata, "Cardiorespiratory responses to passive walking-like exercise in motor-complete spinal cord-injured humans," *Research Bulletin, National Rehabilitation Center for Persons with Disabilities*, vol. 30, pp. 31-37, 2009.

[3] B. Nordström, A. Näslund, M. Eriksson, L. Nyberg, and L. Ekenberg, "The impact of supported standing on well-being and quality of life," *Physiotherapy Canada*, vol. 65, no. 4, pp. 344-352, 2013.

[4] Y. Eguchi, H. Kadone, and K. Suzuki, "Standing mobility vehicle with passive exoskeleton assisting voluntary postural changes," in *Proc. 2013 IEEE/RSJ International Conference on Intelligent Robots and Systems*, pp. 3-7. 2013.

[5] A. Aead, N. Alsamony, and A. El Khateeb, "Multipurpose voice controlled wheelchair," *Journal of Multidisciplinary Engineering Science Studies*, vol. 2, pp. 552-555, 2016.

[6] K. B. Hasnan and L. B. Saesar, "A size-bed wheelchair design with scaled prototype," in *Proc. 2012 International Conference on Industrial Engineering and Operations Management*, pp. 1771-1780, 2012.

[7] Y. S. Yang, M. D. Chen, W. C. Fang, J. J. Chang, and C. C. Kuo, "Sliding and lower limb mechanics during sit-stand-sit transitions with a standing wheelchair," *BioMed Research International*, pp. 1-8, 2014.

[8] S. Suzuki, Y. Matui, M. Takahashi, A. Kakimoto, and Y. Ohta, "Development of a new mobility device, having standing-position walk and seating- position movement," in *Proc. Conference LIFE2010*, vol. 2, pp. 530-531, 2010.

[9] T. Yokoi, A. Takahashi, H. Okada, K. Ohyama, and M. Muraoka, "Estimation of inertia properties of the body segments in Japanese athletes," *Daigaku Shuppan-Kai*, pp. 23-33, 1992.

Tomozumi Ikeda was born in Matsumoto, Japan, on Aug. 1, 1971. He received his Ph.D. degree from the University of Electro-Communications in 2007. He is an associate professor in the Faculty of Human Resources Development at the Polytechnic University of Japan. His primary research interests include life support technology, embodied cognitive science, and development of multimodal interfaces for visually impaired people.

Toshitake Araie was born in Kaga, Japan, on Sep. 19, 1975. He is a 4th-year student in the doctoral program of Tokyo University of Agriculture and Technology. He is an assistant professor in the Faculty of Human Resources Development at the Polytechnic University of Japan. His primary research interests include development of agricultural power assist suits, life support technology, and embodied cognitive science.

Akira Kakimoto was born in Hiroshima, Japan, on Jan. 10, 1962. He graduated from the University of Tokyo in the Department of Precision Machinery Engineering in the faculty of Engineering. He received a master's degree in 1986 and a doctor's degree in 1990 in the Department of Precision Machinery Engineering in the Graduate School of Engineering in the University of Tokyo. He became a research associate in Department of Precision Machinery Engineering in the Institute of Vocational Training (presently, the Polytechnic University of Japan) in 1990. He became an assistant professor in the Department of Mechanical and Control Engineering in 1992, and a professor in mechanical system engineering in 2010. His current interests include assistive technology and machine control. Prof. Kakimoto, is a member of EMBS IEEE, JSPE, JSME, LST, and JSWSAT.

Koji Takahashi was born in Tokyo, Japan, on Nov. 9, 1956. He received the bachelor, master, and doctor degrees in control engineering from the Tokyo Institute of Technology, Japan, in 1980, 1982, and 1985, respectively. He became an assistant professor in the Department of Control Engineering, Tokyo Institute of Technology in 1985, and became an associate professor in the Department of Electrical and Electronic Engineering, Tokyo Institute of Technology in 1991. He has been a professor in the system control engineering unit, Polytechnic University of Japan since 2015. His research interests include system control and smart automation. Prof. Takahashi is a member of SICE, IEEJ, IEICE, and RSJ.